

Whole-field total density measurements by Digital Image Correlation

Alexander M. van Oers · Leo R.M. Maas

Received: date / Accepted: date

Abstract An optical method for the quantitative measurement of the total density field of two-dimensional stratified or homogeneous transparent fluids is presented. It is based on the Synthetic Schlieren method. Application of this method is illustrated by the determination of the static background density of a two-layer fluid and of a stratified fluid. Further aspects of the technique are illustrated by considering the dynamic total density field of a wave attractor in a stratified fluid.

Keywords First keyword · Second keyword · More

1 Introduction

The Background Oriented Schlieren technique (BOS) is an optical density visualization technique [9, 12]. First described in [3], where it was called Synthetic Schlieren (SS). This technique provides whole-field measurements of density gradients. One of the strengths of this technique was the simplicity of the experimental setup. Parts of the traditional, more extensive optical setups were replaced by digital image analysis.

In a typical BOS or SS application, perturbations (waves) in a fluid contained in a tank are imaged. Two or more images are compared using Digital Image Correlation (DIC) [14]. This comparison yields the displacements between the images. These displacements are related to the changes in the gradients of the index of refraction using a ray tracing model. These gradients of the index of refraction are related to the gradients of the density by experimentally determined data (e.g. [15]), by the Gladstone-Dale relation for gases [1] or by the Lorentz-Lorenz

Grants or other notes about the article that should go on the front page should be placed here.

Alexander M. van Oers

NIOZ Royal Netherlands Institute for Sea Research and Utrecht University, P.O. Box 59, 1790 AB Texel, The Netherlands

Present address: Netherlands Defence Academy, The Netherlands

Leo R.M. Maas

Imau, Inst. for Marine and Atmospheric research Utrecht, Utrecht University, Princetonplein 5, 3584 CC, Utrecht, The Netherlands

equation for liquids [6]. The density field is sometimes obtained from the gradients of the density perturbations by solving a Poisson equation [18, 19].

In this paper we present a modification to the BOS or SS technique to directly measure the density field. We take images of static situations: (1) before filling a tank in the experimental setup with (stratified) fluids, (2) after filling the tank with a calibration fluid and (3) after filling the tank with (stratified) fluids. Then we take images of the dynamic situations: we image, as in BOS or SS, the perturbations, or waves, traveling through a fluid. We perform DIC to obtain displacements between the static images. Using a ray tracing model we relate these displacements to the index of refraction. These static images give us the background index of refraction. We follow the same procedure for the dynamic images.

The challenge of this new method is to have enough accuracy in our measurements and models to ensure that our results are useful. Determining the value of the density is more sensitive to noise than determining the density gradients of perturbations in a BOS or SS application. We also want to preserve the experimental simplicity of the BOS or SS method. In Section 2 we perform a naive application of the BOS or SS technique to try to measure the index of refraction of homogeneous water. We analyze a simple ray tracing model to determine why our naive approach failed. We show that light rays, traveling from the background through the fluid to the camera, should not travel in nearly straight lines (as in BOS or SS) but should have large deflections. We should either rotate the fluid tank or rotate (and move) our camera. We should not be placing our camera right in front of the fluid tank.

To obtain the required accuracy in determining the density field we optimize all the steps in our method. In Section 3 we derive our ray tracing model relating displacements to the index of refraction. We call this our forward model: given an index of refraction field and experimental parameters, we can compute the displacement field of our experimental setup. This ray tracing model is a 3D model that allows the camera to be placed under an angle with respect to the fluid tank. In Section 4 we describe our calibration procedure. This calibration determines accurately certain parameters in our forward model. In Section 5 we discuss DIC. We provide references to papers that discuss techniques that allow us to get the most of our DIC procedure. We also provide information about our settings for a typical DIC calculation. In Section 6 we briefly discuss the experimental setup. We also discuss best practices to get the most out of our experiments. In Section 7 we discuss how to solve our inverse model: how to obtain the index of refraction from the experimentally obtained displacements and our forward model.

2 Simple Model

Consider the experimental set up as shown in Figure 1. Light rays travel from a camera, through a water tank onto a background with a random dot pattern. We describe the camera as a pinhole camera. We place the origin of the Cartesian coordinate system at the pinhole, the location where all light rays falling on the ccd sensor pass through. The z -axis is perpendicular to the experimental setup, i.e. such that a light ray traveling along the z -axis will not be refracted by the set-up. We want to determine the position where the light rays ends up, x_6 . The light ray exits the camera with a position $x_1 = 0$ and an angle θ_x .



Figure 1: A schematic view of a path of a light ray (not to scale). The light ray in the reference state is indicated by a solid line, the light ray after filling the tank with water by a dashed line. The numbers indicate the planes through which the light ray propagates: 0, the ccd sensor inside the camera; 1, the camera pinhole; 2, the start of the first glass plate; 3, the end of the first glass plate; 4, the start of the second glass plate; 5, the end of the second glass plate; 6, the screen from which the light rays originate. n_0 , n_1 and n_2 are the index of refraction of, respectively, air, material of the tank and the fluid. The lengths (in the z -direction) are: L_c , the distance from camera to the first glass plate; L_g , the width of the glass plates; L_t the width of the tank; L_s , the distance from the second glass plate to the screen.

Assuming the refractive index in each section of the set up is constant, we can write for the light path,

$$x(z) = x_i + z \tan \theta_i, \quad i = 1, \dots, 5, \quad (1)$$

where x_i is the x -position of the light ray at the start of each section and θ_i is the angle between the direction the ray is propagating and the z -axis. When encountering a discontinuous change in refractive index (when passing between the sections), we invoke Snell's laws

$$n_i \sin \theta_i = \text{constant}, \quad (2)$$

where n_i is the refractive index for the i^{th} section. The position x_6 is

$$x_6(\theta_x, n_2) = (L_c + L_s) \tan \theta_x + \frac{2L_g n_0 \sin \theta_x}{\sqrt{n_1^2 - n_0^2 \sin^2 \theta_x}} + \frac{L_t n_0 \sin \theta_x}{\sqrt{n_2^2 - n_0^2 \sin^2 \theta_x}}. \quad (3)$$

The displacement Δx is the difference in position x_6 between the constant reference state, $n_2 = n_0$, and the unknown state $n_2 = n$,

$$\Delta x = x_6(n_2 = n_0) - x_6(n_2 = n) = L_t \left(\tan \theta_x - \frac{n_0 \sin \theta_x}{\sqrt{n^2 - n_0^2 \sin^2 \theta_x}} \right). \quad (4)$$

Inverting this relation we obtain the unknown refractive index n as a function of the displacement

$$n = \frac{n_0 \sin(\theta_x)}{\tan(\theta_x) - \frac{\Delta x}{L_t}} \sqrt{1 + \left(\tan(\theta_x) - \frac{\Delta x}{L_t} \right)^2}. \quad (5)$$

The angle θ_x , the displacement Δx and unknown index of refraction n are functions of the coordinate x .

Figure 2 shows the results when using (5) to obtain the index of refraction n . We have two frontal images of the experimental setup; (1) Figure 2a, without water, and (2) Figure 2b, with water. Applying DIC we obtain; Figure 2c the correlation coefficient, a measure of the reliability of the method; Figure 2d the horizontal displacements Δx ; and (3) Figure 2e the vertical displacements Δy . Where $\Delta x = \Delta y = 0$ is the location of the z -axis. We calculate the angles θ_x and θ_y with respect to this z -axis. Using (5) we can compute the index of refraction n . Figure 2f shows n obtained from the horizontal displacements Δx . Figure 2g shows n obtained from the vertical displacements Δy . In Figure 2h we combine the horizontal and vertical displacements to obtain n .

We see that when the displacements approach zero, we have very large errors in n . Figure 2h looks best, but is still unacceptable. Around the location of the z -axis, where the angles and displacements approach zero, the errors are very large. The entire figure should have a constant value of $n = 1.333$. This is not the case.


Equations (4) and (5) reveal a problem when determining n : When the angle θ_x goes to zero, (4) shows Δx goes to zero. Then the numerator in the fraction in (5) goes to zero, while the two terms in the denominator both go to zero. So we get large errors in the magnitude of n since we are dividing $0/0$ and we get possibly negative values of n since both terms in the denominator can go to zero. In any measurement we have noise, resulting in uncertainties in Δx and θ_x . These uncertainties have a large effect on the value of n since the expected values of Δx and θ_x are small.

To solve this, we want θ_x to not approach zero. Then, according to (4), Δx does not approach zero and our calculation of n is not plagued by a fraction that approaches $0/0$. To achieve this, we place our camera at an angle α with respect to the water tank. The angle θ_x is replaced by $\alpha + \phi_x$, where ϕ_x is the angle of the light ray relative to the principal axis of the camera, which is at an angle α .

We want Δx to vary with n as much as possible. So, we want n to vary with Δx as little as possible. To find the best angle θ_x to achieve this, we take the derivative of (5) with respect to $\Delta x/L_t$ [10]. Figure 3 show this derivative:




Figure 2: Simple Model Result. Applying DIC to the Reference Image in 2a and the Deformed Image 2b yields the Correlation Coefficient in 2c, the horizontal displacements in 2d and the vertical displacements in 2e. Using (5) the index of refraction n in 2f, 2g and 2h are obtained. When the displacements Δx and Δy approach zero, large errors in n appear.



dndx.png

Figure 3: Derivative of n with respect to $\Delta x/L_t$ as a function of θ_x .



dndt.png

Figure 4: Derivative of n with respect to θ_x as a function of θ_x .

$\partial n / \partial (\Delta x / L_t)$ decreases with increasing θ_x . The worst possible angle to measure Δx is 0° .

Since there is also an uncertainty in the angle, we want n to vary with θ_x as little as possible. Figures 4 show this derivative. The magnitude of this derivative $|\partial n / \partial \theta_x|$ first decreases with increasing θ_x , reaches a minimum, then increases again. The worst possible angles to measure at are 0° and 90° . The minimum is reached at 31° . Any angle between 15° and 55° yields approximately the same sensitivity of n .

Viewing at too large an angle (e.g. 70°) makes it hard to see through the water tank.

Concluding, Figures 3 and 4 indicate that the worst angles to measure are close to zero. Angles between 15° and 55° result in small errors in n .

3 Forward Model

In this section we build a forward model, relating an index of refraction field n , position on the ccd-sensor \underline{x} and parameters $\underline{\alpha}$ to the coordinates \underline{X} where the light rays hits the screen. We seek a model $\underline{X}(n, \underline{\alpha}, \underline{x})$.

In Subsection 3.1 we derive the equations governing 3-dimensional ray optics in an inhomogeneous medium. In Subsection 3.2 give a mathematical description of all the objects our light rays encounter. In Subsection 3.3 we construct the full ray path from the camera through the tank to the screen

3.1 Ray Equation

In this section we derive equations describing the paths light rays follow in inhomogeneous media. Inhomogeneous media have a index of refraction n that varies with position.

A curved ray path is a space curve, which we can describe by a parametric representation, $\underline{r}(\sigma) = (x(\sigma), y(\sigma), z(\sigma))$, where σ is an arbitrary parameter. The two most used parameters are (1) the path length long the ray s and (2) the axial position z . We denote derivatives with respect to the parameter by dots, so $\dot{\underline{x}}(\sigma) = d\underline{x}(\sigma)/d\sigma$. All parameters are functions of s .

The optical length \mathcal{A} of a path $\underline{r}(s)$ taken by a ray of light passing from point A to point B in three-dimensional space is defined by

$$\mathcal{A} = \int_A^B n(\underline{r}(s)) ds, \quad (6)$$

where $n(\underline{r})$ is the index of refraction at the spatial point $\underline{r} \in \mathbb{R}^3$. We choose the element of arc length ds along the ray path $\underline{r}(s)$ through that point as $ds^2 = d\underline{r}(s) \cdot d\underline{r}(s)$, so that $|\dot{\underline{r}}| = 1$.

Applying Fermat's principle [4] yields the eikonal equation for ray optics

$$\frac{\partial n}{\partial \underline{r}} = \frac{d}{ds} \left(n(\underline{r}) \frac{d\underline{r}}{ds} \right). \quad (7)$$

Only two of the component equations are independent, since $|\dot{\underline{r}}| = 1$.

To find the equations used in Synthetic Schlieren [20, 3], we first derive the axial eikonal equation. Most optical instruments are designed to posses a line of sight (or primary direction of propagation of light) called the optical axis. In Synthetic Schlieren this optical axis coincides with the direction in which the refractive index n does not vary. Choosing a Cartesian coordinate system such that the z -axis coincides with this optical axis, expresses the arc-length ds in terms of the increment along the optical axis, dz . Our parametric description is now in terms of z : $\underline{r}(z) = (x(z), y(z), z)$. From our definition of ds

$$ds(z) = \sqrt{dx^2(z) + dy^2(z) + dz^2} = \sqrt{1 + \dot{x}^2 + \dot{y}^2} dz = \frac{1}{\gamma} dz, \quad (8)$$

where $\dot{x} = dx/dz$ and $\dot{y} = dy/dz$ and

$$\gamma = \frac{dz}{ds} = \frac{1}{\sqrt{1 + \dot{x}^2 + \dot{y}^2}} = \cos \theta \leq 1, \quad (9)$$

where θ is the angle the ray makes with the z -axis. Using (9) in (7) yields the axial eikonal equation

$$\gamma \frac{d}{dz} \left(n(\underline{r}(z)) \gamma \frac{d\underline{r}(z)}{dz} \right) = \frac{\partial n(\underline{r}(z))}{\partial \underline{r}}. \quad (10)$$

This yields three equations, one for each coordinate direction,

$$\ddot{x} = \frac{1}{\gamma^2} \frac{1}{n} \left(\frac{\partial n}{\partial x} - \dot{x} \frac{\partial n}{\partial z} \right), \quad \ddot{y} = \frac{1}{\gamma^2} \frac{1}{n} \left(\frac{\partial n}{\partial y} - \dot{y} \frac{\partial n}{\partial z} \right), \quad \frac{\partial n}{\partial z} = \gamma \frac{d}{dz} (n\gamma). \quad (11)$$

Indeed, this system of equations shows that only two equations are independent. In Synthetic Schlieren the variation in n in the z -direction, the optical axis, is assumed to be zero. Then (11) reduce to

$$\ddot{x} = \left(1 + \dot{x}^2 + \dot{y}^2 \right) \frac{1}{n} \frac{\partial n}{\partial x}, \quad \ddot{y} = \left(1 + \dot{x}^2 + \dot{y}^2 \right) \frac{1}{n} \frac{\partial n}{\partial y}, \quad (12)$$

which are the starting point for the derivation of Synthetic Schlieren in [3].¹

In the application presented in this paper, the optical axis does not coincide with the direction in which the refractive index n does not vary. Our parametric description is in the arc-length s and not in z . We cannot solve (7) analytically, so we solve it numerically. We first write our system of three second-order differential equations as a system of 6 first-order differential equations by introducing a quantity \underline{T} [13] such that (7) becomes

$$\frac{d\underline{r}}{ds} = \frac{\underline{T}}{n}, \quad \frac{d\underline{T}}{ds} = \nabla n. \quad (13)$$

We apply a Runge–Kutta fourth-order method to solve this system.

3.2 Mathematical description of Geometrical Objects

To give our method flexibility and not making assumption on the relative configuration in our experimental setup, we model the light rays as traversing in a three-dimensional space and allow the different elements in the experimental setup to have any alignments.

We place our origin again at the pinhole. The z -axis aligns with the optical axis of the camera, i.e. the viewing direction of the camera. All the light entering the camera travels through the pinhole and falls on the ccd-sensor. The x - and y -axes span a plane through the origin parallel to this ccd-sensor.

¹ The third equation in (11) reduces to $n\gamma = \text{constant}$. To integrate (12) we do not need to assume \dot{x} and \dot{y} are small. Experimentally, this means we can apply Synthetic Schlieren even when the angles of the light rays are large.

3.2.1 Plane Definition

The mathematical definition of a plane is

$$\hat{n} \cdot (\underline{x} - \underline{x}_0) = 0, \quad (14)$$

where $\hat{n} = (a, b, c)$ is the unit normal vector of the plane, \underline{x} a random vector within the plane and $\underline{x}_0 = (x_0, y_0, z_0)$ a random point on the plane. Expanding (14) yields

$$ax + by + cz + d = 0 \quad \text{with} \quad d = -ax_0 - by_0 - cz_0. \quad (15)$$

For each of the planes 2 to 6 in Figure 1, we can write an equation of the form (15). We assume all planes are parallel to each other. Then the parameters a , b and c are the same for each plane; only d changes. The distances in the normal direction of each plane are known, e.g. L_s , L_g , etc. Given the equation describing plane 6, with $d = d_6$, we can compute the equations describing the other planes

$$\begin{aligned} ax + by + cz + d_i &= 0, & d_5 &= d + (a + b + c)L_s, \\ &\dots, \\ d_2 &= d + (a + b + c)(L_s + 2L_g + L_t), \\ d_1 &= d + (a + b + c)(L_s + 2L_g + L_t + L_c) = 0 \end{aligned} \quad (16)$$

3.2.2 Direction Cosines

Each pixel in our image corresponds to a physical location on the ccd-sensor with coordinates $\underline{x} = (x, y, -L_f)$, where L_f is the distance from the ccd-sensor to the pinhole in the z -direction. We calculate this distance with the thin lens equation

$$\frac{1}{L_f} + \frac{1}{L_m} = \frac{1}{f}, \quad (17)$$

where f is the focal length of the camera and L_m is the distance from the pinhole to screen (plane 6) along the z -axis. This distance is found from (15) for $x = y = 0$. Then $d = -cL_m$.

The physical coordinates x and y are obtained from the pixel locations x_p, y_p and the physical size of each pixel on the ccd-sensor. Assuming each pixel on the ccd-sensor is square, we call the physical size of each sensor S_p^2 . S_p has units $\mu\text{m}/\text{pixel}$. The physical coordinates are then found from the pixel locations by

$$x = S_p(x_p - x_p^0), \quad y = S_p(y_p - y_p^0), \quad (18)$$

where x_p^0 and y_p^0 are the pixel locations at $(x, y) = (0, 0)$.

Each light ray travels in a straight line from these coordinates \underline{x} , through the pinhole, to the experimental setup. We describe each of these light rays with direction cosines: the cosines of the angles between the light ray and the three coordinate axes:

$$\begin{aligned} \alpha = \cos \theta_x &= \frac{x}{\sqrt{x^2 + y^2 + L_f^2}} & \beta = \cos \theta_y &= \frac{y}{\sqrt{x^2 + y^2 + L_f^2}} \\ \gamma = \cos \theta_z &= \frac{L_f}{\sqrt{x^2 + y^2 + L_f^2}} \end{aligned} \quad (19)$$

At the pinhole, all light rays pass through the origin and have coordinates $(0,0,0)$. Each light ray has direction cosines (α, β, γ) .

3.2.3 Intersection Light Rays and Planes: Homogeneous medium

The equation governing light rays in homogeneous media is

$$\underline{p} = \underline{s} + \underline{I}l, \quad (20)$$

where $\underline{s} = (s_x, s_y, s_z)$ is the initial position, $\underline{I} = (\alpha, \beta, \gamma)$ the direction cosines, $\underline{p} = (p_x, p_y, p_z)$ the final position and l the length traveled along the light ray.

To intersect with a plane, the final position \underline{p} must lie on that plane. Substituting (15) into (20) and solving for l yields

$$l = -\frac{d + as_x + bs_y + cs_z}{a\alpha + b\beta + c\gamma} \quad (21)$$

Substituting this l into (20) yields the location where each light ray intersects with the plane.

3.2.4 Snell's Law

To find the angle of incidence, θ_I , between the incoming light ray and the plane, we compute

$$\cos \theta_I = \hat{n} \cdot \underline{I}. \quad (22)$$

We apply Snell's law (2) to find the angle of refraction, θ_T . The index of refraction of the medium through which the incoming ray travels is n_I , the index of refraction of the medium through which the outgoing ray travels is n_T . To find the direction cosines of the outgoing ray, \underline{T} , we calculate

$$S = \text{sign} \cos \theta_I, \quad \sin \theta_T = \frac{n_I}{n_T} \sqrt{1 - \cos^2 \theta_I}, \quad (23)$$

$$\cos \theta_T = \sqrt{1 - \left(\frac{n_I}{n_T}\right)^2 (1 - \cos^2 \theta_I)} \quad \underline{T} = \frac{n_I}{n_T} \underline{I} + \left(\frac{n_I}{n_T} \cos \theta_I - S \cos \theta_T\right) \hat{n}, \quad (24)$$

where S , the sign of $\cos \theta_I$ ensures we stay in the right quadrant.

3.3 Displacements

Previous subsections combine to give the forward model: $\underline{X}(n, \underline{\alpha}, \underline{x})$. Given an index of refraction field n , parameters $\underline{\alpha}$ and coordinates $\underline{x} = (x, y)$, we can calculate the location on the screen where the light rays end up. $\underline{\alpha}$ are the parameters that define the planes a, b, c and the distance to the screen L_m . We use L_m instead of d since we want our parameters to be (linearly) independent. Also, L_m has a clear geometric meaning.

We take our forward model twice, once for a known index of refraction (typically constant) n_0 and once for an unknown index of refraction field n . The light rays originating from the same location on the screen end up on different locations on the ccd sensor:

$$\underline{X}(n, \underline{\alpha}, \underline{x} + \underline{\Delta x}) - \underline{X}(n_0, \underline{\alpha}, \underline{x}) = 0, \quad \underline{X} = (X, Y, Z). \quad (25)$$

This equation holds for each measured displacement $\underline{\Delta x} = (\Delta x, \Delta y)$. From (19) we see that light rays with different locations on the ccd-sensor have different angles with which they leave the camera. Due to the different index of refraction in the tank, they do end up in the same location on the screen.

4 Calibration

In our forward model in Section 3.2, we have used the parameters $\underline{\alpha}$. However, when setting up a new experiment, these are not known. To obtain these, we perform a calibration step. This calibration determines the parameters very precisely and gives us a lot of experimental freedom. For example, we do not have to align the camera, or even measure the position of the camera relative to the water tank. We use calibration for this.

The calibration consists of performing one extra measurement (two in total): we take a reference image, the tank without water (filled with air) and a deformed image, the tank filled with water with a known index of refraction. The easiest is water without any salts. Performing DIC yields us the displacements $\underline{\Delta x}$. This allows us to determine the parameters $\underline{\alpha}$.

Looking at our Forward Model (25), we know

1. $n = n_0$ and $n = n_1$, the index of refraction of the reference image (filled with air) and the deformed image (filled with water);
2. \underline{x} , the coordinates on our ccd-sensor;
3. $\underline{\Delta x}$, the measured displacement (after DIC).

The unknowns are the parameters $\underline{\alpha} = (a, b, c, L_m)$. Since we have only four parameters to estimate and many measurements (each grid point yields a separate equation), we have an over-determined system. We use least-squares to find those $\underline{\alpha}$ that minimize the sum of squares of the residuals. The forward model depends nonlinearly on the parameters $\underline{\alpha}$ and the measurements $\underline{\Delta x}$. For each measurement $\underline{\Delta x}$ we have a measure of reliability, the correlation coefficient, which we use as a weight w in the least squares procedure

$$\min_{\underline{\alpha}} \sum_i w_i (X_j(n_1, \underline{\alpha}, \underline{x}_i + \underline{\Delta x}_i) - X_j(n_0, \underline{\alpha}, \underline{x}_i))^2, \quad (26)$$

with constraints (1) $L_c > 0$ and (2) $L_m \geq L_c + 2L_g + L_t + L_s$, the experimental setup is in front of the camera; (3) $c < 0$, the unit normal vector of the planes points in the negative z -axis. Combining these constraints implies $d > 0$. The sum is over all measured displacements. We use only the displacements in the x -direction, since that is the direction with the largest angles and thus largest signal.

The distance L_c between the camera and the front of water tank (plane 2) along the \hat{n} direction is obtained from the total distance d between the camera and the screen along the z -direction and the distances L_g , L_t and L_s . This ensures internal consistency in our model. We obtain L_c from (16).

We use the Levenberg-Marquardt (LM) algorithm to solve (26). Generally, (26) has one minimum that satisfies the constraints. When the initial condition satisfies these constraints, the LM algorithm will find this minimum.

5 Digital Image Correlation

Digital Image Correlation (DIC) is a well known technique [14] to obtain deformation maps from images. We use second-order shape functions [7] to handle large nonlinear deformations. To attain sub-pixel accuracy we interpolate our images with B-splines [16, 17]. To obtain the deformations we optimize a Correlation Coefficient, the ZNSSD [14]. We solve this nonlinear least-squares problem by (1) providing an initial guess and (2) solving an iterative scheme. As an initial guess we perform Template Matching [5, 2] on a limited set of points to obtain rigid deformations with pixel accuracy. After applying DIC to obtain sub-pixel deformations, we use reliability guided DIC [11] with a propagation function [21] to determine the initial guesses. As iterative scheme we use the LM algorithm.

Table 1: Digital Image Correlation parameters.

Noise	
Subset Size	
Grid Size	5
Measurements Points	
Total Number of Images	
Number of Averaged Images	
Displacements	
Spatial Resolution	x pixels, x mm
Resolution	0.0105 pixels (x mm)
Index of Refraction	
Smoothing Method	
Resolution	x

Table 1 shows the typical DIC parameters used in our experiments. Additionally, the accuracy of the obtained displacements is given.

6 Experimental

Best practices to get good quality images [14]

random dot pattern -i grey -i histogram no over/under saturation

7 Inverse Model

Looking at our Forward Model (25), we know

1. $\underline{\alpha}$, the parameters of our experimental setup (after calibration),
2. \underline{x} , the coordinates on our ccd-sensor,
3. $\underline{\Delta x}$, the measured displacement (after DIC),
4. n_0 , the index of refraction of the reference state.

The unknown is the index of refraction field n . Unlike the simple model (5), we cannot invert the forward model to obtain an expression for the index of refraction n . We treat the problem of finding n as an optimization problem:

$$\min_{n_i} (X_j(n_i, \underline{\alpha}, \underline{x}_i + \underline{\Delta x}_i) - X_j(n_0, \underline{\alpha}, \underline{x}_i))^2, \quad (27)$$

with constraints $1.333 \leq n_i \leq 1.4$. For each measurement $\underline{\Delta x}_i$ we solve (27) to find n_i . We solve (27) with the LM algorithm. (27) has one minimum in the range $1.333 \leq n_i \leq 1.4$. Picking an initial condition in this range ensures LM finds this minimum.

Since we are working with liquids we use the Lorentz-Lorenz equation to relate the index of refraction n to the density ρ [6, 15],

$$\frac{n^2 - 1}{n^2 + 2} \frac{1}{\rho} = \text{constant}. \quad (28)$$

We use our calibration measurement to determine the constant: $\rho = 1$ for $n = 1.333$.

8 Results

In this section we show three applications of the new method: (1) A static two-layer fluid with large nonlinear deformations, (2) A static stratified fluid and (3) a dynamic fluid/flow? with wave attractor.

In the first application, Figure 5, we measured the background density of a two-layer fluid system. We filled the bottom half of a tank with Wadden Sea water (with an index of refraction of 1.338)² and the upper half of the tank with tap water (with an index of refraction of 1.333). We kept the interface between the two layers sharp by filling the upper half of the tank through a sponge. The observed deformations of the dot pattern through this interface are large. Through the use of the second-order shape functions in the DIC procedure, we can still determine these deformations. Figure 5g shows the index of refraction field n . The expected theoretical density profile is an error function. We see this in Figure 5g.

Table 2: Angles β of internal wave beams as a function of the forcing frequency ω . These were determined by a Synthetic Schlieren setup.

ω	1	1	1	1	1
β	1	1	1	1	1

In the second application, Figure 5, we measured the background density of a continuously stratified fluid. We filled a tank through the double bucket method. After taking a Reference Image, a Calibration Image and a Deformed Image, we repositioned the camera for a Synthetic Schlieren measurement. After oscillating the tank, we measured the angles of the internal waves propagating in the fluid. Table 2 shows the forcing frequencies ω and angles β . Through

$$N = \omega \cos \beta \quad (29)$$

we determined the buoyancy frequency N . Through

$$N^2 = -\frac{g}{\rho_0} \frac{d\rho_0}{dz} \quad (30)$$

- (a) Reference Image: Filled with air (b) Calibration Image Image: Filled with water with known n
- (c) Deformed Image: Filled with salt water with unknown n -field (d) Index of Refraction n for Calibration Image
- (e) Δx from DIC (f) Δy from DIC
- (g) Index of Refraction n for Deformed Image (h) Correlation Coefficient from DIC
- (i) n profiles for Calibration and Deformed Images

Figure 5: The procedure for obtaining the index of refraction field n . We obtain three images: one Reference Image (5a) filled with air, one Calibration Image (5b) filled with water without salts and one Deformed Image (5c) filled with water with an unknown n -field. Applying DIC between the Reference Image and the Calibration image, we find the displacements $D = (\Delta x, \Delta y)$. Using these displacements D in (26), we obtain the parameters $\underline{\alpha}$. After calibration, the resulting n -field is uniform (5d). Applying DIC between the Reference Image and the Deformed Image, we find the displacements Δx (5e) and Δy (5f) with corresponding Correlation Coefficient (5h). Using these displacements in (27), we obtain the unknown index of refraction field n (5g). Horizontally averaging the index of refraction fields n yields the profiles in 5i.

- (a) Deformed Image: Filled with salt water with unknown n -field (b) Correlation Coefficient from DIC
- (c) Δx from DIC (d) Δy from DIC
- (e) Index of Refraction n for Deformed Image (f) Background Density ρ_0 for Deformed Image

Figure 6: Determining the background density for a continuously stratified fluid. After taking three images, with the Deformed Image 6a, we obtain the displacements Δx in Figure 6c and Δy in Figure 6d from DIC. After calibration we obtain the index of refraction field n in Figure 6e. Using the Lorentz-Lorenz relation we obtain the density profile 6f with buoyancy frequency N of NUMBER.

we determined the buoyancy frequency N , obtained from our new method.

In the third application, we measured the density field of a wave attractor [8]. Figure 7 shows the measured density fields over one period of a (1,1) Wave Attractor.

9 Discussion

definition planes - \hat{z} doesn't have to be parallel. in particular 6th plane can be different, extra parameters to estimate in α (calibration). non plane water tank: measure without tank, with tank with air - \hat{z} (calibration) shape of tank, field L_t - \hat{z} doesn't even have to be planes

² Measured by a refractometer: The Atago Urine Specific Gravity Refractometer with a refractive index range of 1.333-1.356 and a resolution of 0.0005.

(a) 0	(b) P/6
(c) P/3	(d) P/2
(e) 2P/3	(f) 5P/6

Figure 7: Density Fields over one period of a Wave Attractor. The forcing frequency was NUMBER.

Same experimental equipment as BOS or SS - Can apply this method. All complexity is in the image analysis.

Need to say something about paraxial approximation

The two novel critical steps are: (1) To view the experimental setup under an angle and (2) To calibrate our model.

Horizontal viewing $\Rightarrow \Delta x, \theta_x$ large. Use $X \Rightarrow \frac{\partial n}{\partial x} = 0$ in static situation.

Acknowledgements If you'd like to thank anyone, place your comments here

Funding

NWO

Availability of data and material

Code availability

Conflict of interest

The authors declare that they have no conflict of interest.

References

- [1] Max Born and Emil Wolf. *Principles of optics: electromagnetic theory of propagation, interference and diffraction of light*. Elsevier, 2013.
- [2] G. Bradski. "The OpenCV Library." In: *Dr. Dobb's Journal of Software Tools* (2000).
- [3] SB Dalziel, Graham O Hughes, and Bruce R Sutherland. "Whole-field density measurements by 'synthetic schlieren'." In: *Experiments in fluids* 28.4 (2000), pp. 322–335.
- [4] Darryl D Holm. *Geometric mechanics: Part I: Dynamics and symmetry*. World Scientific Publishing Company, 2011.
- [5] JP Lewis. "Industrial Light & Magic." In: *Fast normalized cross-correlation* 2011 (1995).
- [6] Hendrik Antoon Lorentz. *The Theory of Electrons and Its Applications to the Phenomena of Light and Radiant Heat: A Course of Lectures Delivered in Columbia University, New York in March and April, 1906*. Vol. 29. Teubner, 1916.

- [7] H Lu and PD Cary. “Deformation measurements by digital image correlation: implementation of a second-order displacement gradient.” In: *Experimental mechanics* 40.4 (2000), pp. 393–400.
- [8] Leo RM Maas et al. “Observation of an internal wave attractor in a confined, stably stratified fluid.” In: *Nature* 388.6642 (1997), pp. 557–561.
- [9] GEA Meier. “Computerized background-oriented schlieren.” In: *Experiments in fluids* 33.1 (2002), pp. 181–187.
- [10] Shojiro Nemoto. “Measurement of the refractive index of liquid using laser beam displacement.” In: *Applied optics* 31.31 (1992), pp. 6690–6694.
- [11] Bing Pan, Wu Dafang, and Xia Yong. “Incremental calculation for large deformation measurement using reliability-guided digital image correlation.” In: *Optics and Lasers in Engineering* 50.4 (2012), pp. 586–592.
- [12] Markus Raffel. “Background-oriented schlieren (BOS) techniques.” In: *Experiments in Fluids* 56.3 (2015), p. 60.
- [13] WH Southwell. “Ray tracing in gradient-index media.” In: *JOSA* 72.7 (1982), pp. 908–911.
- [14] Michael A Sutton, Jean Jose Orteu, and Hubert Schreier. *Image correlation for shape, motion and deformation measurements: basic concepts, theory and applications*. Springer Science & Business Media, 2009.
- [15] Chan-Yuan Tan and Yao-Xiong Huang. “Dependence of refractive index on concentration and temperature in electrolyte solution, polar solution, non-polar solution, and protein solution.” In: *Journal of Chemical & Engineering Data* 60.10 (2015), pp. 2827–2833.
- [16] P. Thévenaz, T. Blu, and M. Unser. “Interpolation Revisited.” In: *IEEE Transactions on Medical Imaging* 19.7 (July 2000), pp. 739–758.
- [17] Michael Unser. “Splines: A perfect fit for signal and image processing.” In: *IEEE Signal processing magazine* 16.6 (1999), pp. 22–38.
- [18] L Venkatakrishnan and GEA Meier. “Density measurements using the background oriented schlieren technique.” In: *Experiments in Fluids* 37.2 (2004), pp. 237–247.
- [19] Lilly Verso and Alex Liberzon. “Background oriented schlieren in a density stratified fluid.” In: *Review of Scientific Instruments* 86.10 (2015), p. 103705.
- [20] FJ Weyl. “Analysis of optical methods.” In: *Physical measurements in gas dynamics and combustion*. Princeton University Press, Princeton, New Jersey (1954), pp. 3–25.
- [21] Yihao Zhou and Yan Qiu Chen. “Propagation function for accurate initialization and efficiency enhancement of digital image correlation.” In: *Optics and Lasers in Engineering* 50.12 (2012), pp. 1789–1797.